Arch. Metall. Mater. **63** (2018), 2, 697-707

DOI: 10.24425/122396

M. TEZEGHDENTI*,***#, N. ETTEYEB*,**, L. DHOUIBI*, O. KANOUN***

SUSTAINABLE USE OF NATURAL RESOURCES AS ALTERNATIVE FOR THE HAZARDOUS CORROSION INHIBITOR OF MILD STEEL/DILUTE SULFURIC ACID INTERFACE: WEIGHT LOSS, EIS, AFM AND FTIR STUDIES

Point of present exploration was to figure out the anticorrosion activity of Acacia Cyanophylla (Saligna leaves) extract on the corrosion of mild steel in dilute sulfuric acid medium, using weight loss measurements and electrochemical impedance spectroscopy. The result of the study revealed that the extract act as a potent inhibitor on mild steel in acid medium. The increase in inhibitor concentration and immersion time showed a positive effect on inhibition efficiency. EIS exhibited one capacitive loop which indicates that the corrosion reaction is controlled by charge transfer process. The increase of phase shift (*n*) in presence of (ACLE) lower surface roughness. This change reveals the adsorption of the inhibitor compound on the steel surface. According to the results of weight loss measurements, the adsorption of the extract on the steel surface can be described by the Langmuir isotherm.

The inhibition mechanism of (ACLE) molecules involves physical interaction between the inhibitor and metal surface. Additionally, Protective film formation against acid attack was confirmed by FT-IR and AFM techniques.

Keywords: Acacia Cyanophylla; Inhibition; Corrosion; mild steel; Electrochemical impedance spectroscopy; adsorption; AFM

1. Introduction

Studies corrosion inhibition of metals in acidic media, particularly mild steel corrosion and its inhibition in sulfuric acid is of interest in many industries. Indeed, mild steel has obtained adaptable material, attributable primarily to it's not expense and easy to manufacture for example, in the form of plates, bars and tubes [1]. On the other hand, the most popular mineral acids used to clean the ferrous alloys and some stainless steels having less than 10% chrome and nickel are hydrochloric and sulfuric acid. This is because their high ionization, can be used at room temperature, and are much cheaper (especially sulfuric) than the weaker organic acids. The poor corrosion resistance of mild steel in acid is a major constraint in its applications. Sulfuric acid, in different concentrations, after dissolving the scale, it can weaken the steel [2], enhancing corrosion possibility and leading to economic losses.

Overcoming these problems, there are many approaches that may be applied to protect or minimize the amount of mild steel dissolved. This has been intended by the existence of inhibitors in solution [3,4]. However, the known dangerous effect of most synthetic corrosion inhibitors has motivated scientists to develop cheap, non-toxic and sustainable inhibitors from natural sources [5,6].

Currently, several studies have investigated the corrosion inhibitors for steel especially in acid medium by various plant such as Terminalia catalpa extract [7], mustard seed extract [8], Hibiscus sabdariffa extract [9], Ruta graveolens [10], gongronema latifoliunm [11], Camellia Sinensis leaves [12], alkaloids extract from Molasses plant [13], etc. These researches have revealed that phytochemical compounds containing anchoring group including (N, S and O), that can deposited as a film on a metal surface and provide good protection against corrosive attack.

Also some organic dyes like thymol alizarin yellow GG (AYGG) [14] and blue (TB) [15], were noticed, as non-toxic synthetic corrosion inhibitors, on ferrous metals in sulfuric acid bath.

A restricted number of work have investigated the effect of plant rich in tannin on various metals like mild steel, copper, and aluminum in aggressive solution. As far back as 1964, the beginning of scientific approach on the corrosion inhibition effects of mimosa tannin was published by Booth and Mercer [16]. The investigation of plant extracts rich in tannin was extensively developed in the 21st century. According to Rahim et al, the mangrove (Rhizopora apiculata) tannin extracted from the bark was found to be an excellent potential corrosion inhibitor for steel in acid medium [17].

In an another study carried out by Makanjuola et al, the tannin extract from Rhizophora Racemosa has been investigated as corrosion inhibitor for mild steel in acid medium and found them as efficient inhibitors [18].

* UNIV. TUNIS EL MANAR, U.R .MECANICAL-ENERGETIC NATIONAL SCHOOL OF ENGINEERS OF TUNIS, BP37, LE BELVÉDÈRE 1002, TUNIS, TUNISIA
** HIGHER INSTITUTE OF APPLIED BIOLOGY OF MEDENINE, ROUTE EL JORF , EL FJA 4111, B.P.522, UNIVERSITY OF GABES, TUNISIA
*** TECHNISCHE UNIVERSITAT CHEMNITZ, CHAIR FOR MEASUREMENT AND SENSOR TECHNOLOGY, REICHENHAINER STRASSE 70, 09126 CHEMNITZ, GERMANY
# Coresponding autors; mohamedteze@gmail.com

As recent researches, the use of Tannin as a corrosion inhibitor has been widely investigated. Mimosa tannin extract obtained from the bark of (A. mearnsii) has been considered as a corrosion inhibitor for aluminum alloy in an acid rain solution. The constituent of the extracts creates a barrier for mass and charge transfer, noticeably slowed down the corrosion process [19]. Abu Talib et al [20], used the Tannin bark from Melalauca Cajuputi Powell , it has been discussed that in HCl, bark Gelamwas an effective inhibitor against mild steel corrosion, the rate of corrosion decrease with the increase of concentration.

In pursuit of natural product rich in tannin extracted by simple procedures, A. Cyanophylla (Fabaceae) is leguminosae species belonging from subfamily Mimosoideae [21], native to West Australia [22].

This shrub was introduced in Tunisia for over a century, particularly in the semiarid and arid zones [23]. First, to serve the rangeland rehabilitation, due to the presence of 100-140 g crude protein/kg DM with a high levels of tannins CT (40-80 g Eq leucocyan/kg dry matter) [24]. Then it is used in antibacterial [25], and anti inflammatory [26] activities. In recent years, hot acid extracts of Acacia Cyanophylla leaves harvested from the coastal region of Mersin-Turkey has been studied as a corrosion inhibitor for mild steel in acid condition by electrochemical and Gasometric methods. The results suggest that this extract as a original ecological substance due to its acceptable characteristics for this application [27].

In another case, the phytochemical analysis of Acacia Cyanophylla leaves has been proposed, the last consists primarily of many polyphenols and their acidic compounds [28-30].

It is well known also that some plant polyphenols may be difficultly soluble in water, in the natural state polyphenol-polyphenol interactions usually ensure some minimal solubility in aqueous media [31]. In a previous study [32], A. Cyanophylla extract (ACLE) was investigated as corrosion inhibitor for steel in sulfuric acid solution under the same test conditions as used in the present work. The results obtained were encouraging and that necessitated this renewed interest to further assess to the stability and persistence films adsorbed on the surface.

In this article, the authors investigated the anticorrosion potential of this extract using weight loss and electrochemical impedance spectroscopy. We have also studied the effect of immersion time (up to 36 h) and acid concentration (1-2.0 M H_2SO_4) on inhibition effect of the extract. A probable inhibition mechanism is proposed for this work.

2. Experimental section

2.1. Specimen preparation

In the present mild steel sheet of composition (wt%): 0.14C,0.3Mn, 0.01 Si, 0.02 P, 0.05S and rest being Fe were used in this investigation.

The sheet was mechanically pressed cut into different coupons, each of dimension, 2×2×0.3 cm were used for weight loss measurements. The specimens were embedded in epoxy resin leaving a working area of 0.28 cm^2 used as working electrode in electrochemical measurement.

All plates were abraded by using SiC abrasive papers (Grade No: 220, 400, 600, 800 and 1200), then washed with distilled water and dried in air before each experiment in the corrosive medium.

2.2. Processing of the plant materials

Leaves samples of Acacia Cyanophylla were collected from the Arid Region situated in the south east of Tunisia. The leaves were dried and stored in the laboratory at room temperature and in the shade before the extraction. Dried powder (10 g) was soaked in bidistilled water (100 mL) ratio of 10 mL/g with mechanical agitation at constant stirring rate (200 rpm) for 3 h [32]. The aqueous solution was filtered under vacuum and concentrated to 100 ml. The sample then stored air tight in the refrigerator (4°C) until just before testing to minimize any possible biological activity. From the weight of the dried aqueous fraction, it is calculated as each milliliter of plant extract contains 10 mg of plant compounds. The required concentrations of solution were prepared by using dilution methods in dilute sulfuric acid.

2.3. Corrosion measurements

2.3.1. Weight loss method

Finely polished and dried mild steel coupons were weighed on a digital balance with sensitivity ±0.1 mg, after the specimens were immersed (complete immersion) in a beaker containing 100 ml of test solution at 25°C with a precision of ±0.5°C and left exposed to air.

The corroded/inhibited specimens were washed with distilled water, dried with a hot air stream and reweighed.

The weight loss was calculated as the difference in weight of the specimen before and after immersion in corrosive medium according to the method described previously [33].

The tests were performed in triplicate to guarantee the reliability of the results, and the mean value of the weight loss is reported. The reproducibility of the experiment was higher than 95%. From the weight loss values, corrosion rates (CR_w) in mg cm^{-2} h^{-1} was calculated from the following equation [34-36]:

$$CR_w = \frac{W}{St} \tag{1}$$

where ΔW is average weight loss, s the total area of the specimen, and t is the immersion time. From the corrosion rate thus obtained, the inhibition efficiency (ηw) was calculated as follows:

$$\eta w(\%) = \frac{C_R^0 - C_R}{C_R^0} \times 100 \tag{2}$$

where C_R^0 and C_R are the corrosion rates of mild steel specimens in the absence and presence of inhibitor, respectively.

2.3.2. Electrochemical Studies

Electrochemical impedance spectroscopy (EIS) were carried out in a conventional three-electrode electrolysis cylindrical Pyrex glass cell of 100 mL capacity. A 1 cm^2 platinum foil was used as counter electrode, a saturated calomel electrode (SCE) and mild steel were used as reference and working electrode, respectively. Measurements were carried using VoltaLab 40 model electrochemical Workstation in a frequency range from 65 kHz to 0.01 Hz at five points per decade, with signal amplitude of 10 mV peak-to-peak.

The experiments were measured after 2 h immersion at OCP values without bubbling at room temperature. EIS data was analyzed by ZSimpWin program. The above procedures were repeated three times with success for each concentration of the tested plant extract.

2.4. Fourier-transform infrared (FT-IR) spectroscopy

FT-IR spectra were recorded in an SHIMADZU-FTIR-8400S spectrophotometer, at a frequency range of 4000 to 400 cm^{-1}, using the KBr disk technique. The dried sample of Acacia Cyanophylla leaves was mixed with KBr and made the disk.

The mild steel specimen of size 2×2×0.3 cm was prepared as described above (Section 2.3.1). After immersion in 1.0 M H_2SO_4 with addition of 200 ppm of ACLE at 25°C for 24 h, the specimen was cleaned with distilled water, dried with a cold air blaster. Then the thin adsorption product formed on steel surface was mixed with KBr, and making the pellets.

2.5. Atomic force microscopy analysis

The surface morphology of mild steel specimens after exposure with 1 M H_2SO_4 in the absence and presence optimized inhibitor concentration was studied by an atomic force microscope (AFM) model Agilent 5600 LS, with WSxM software used for image rendering.

3. Results and discussion

3.1. Weight loss measurements

In pickling process with sulfuric acid, the solubility of iron oxides in these acids is not very high. It relies on the relative solubility of the underlying FeO and Fe metal then attacking the base metal.

Scale formed on carbon steels consists of a number of oxide layers whose compositions are determined by the scale formation conditions [37]. A wustite layer (FeO) is adjacent to the metal; the intermediate layer consists of magnetite (Fe_3O_4), while the external layer consists of hematite (Fe_2O_3) [38]. At greater thermodynamic stability, the scale formed was Fe_2O_3 and Fe_3O_4 (intermediate layer between Fe_2O_3 and FeO).

At the outer surface, the mechanism of pickling acid can be explained by considering the following mechanism :

$$Fe_2O_3+2[H] = 2FeO + H_2O \quad (3)$$

$$Fe_3O_4+2[H] = 3FeO + H_2O \quad (4)$$

The mechanism of pickling acid can be explained by considering the following mechanism :

$$FeO + 2H^+ \rightarrow Fe^{2+} + H_2O \quad (5)$$

When the scale is eliminated from the steel surface, protons react with the base steel:

$$Fe + 2H^+ \rightarrow Fe^{2+} + H_2\,(g) \quad (6)$$

An over-pickled steel surface, iron cations can further combine with sulfate ions to form $FeSO_4$. The protective layer ($FeSO_4$) in dilute sulfuric acid is soft poorly adherent, which means that it can be easily damaged [39].

For this purpose a corrosion inhibitor is introduced into the solution to decrease the metal losses considerably.

Weight loss method of monitoring corrosion rate and inhibition efficiency is useful because of the simplicity and this has been employed by several researchers [36,40].

To study the effect of addition of Acacia extract (ACLE) on the inhibition efficiency, weight loss experiments were carried out in three different concentrations of H_2SO_4 at 298K for 24 h immersion period. The values of percentage inhibition efficiency

TABLE 1

Weight loss data of mild steel with and without (ACLE) at various concentrations of H_2SO_4 solutions

Acid conc. (N)	Inh. conc. (ppm)	ΔW (g)	CR_w ($mg.cm^{-2}.h^{-1}$)	ηw (%)	θ
	Blank	0.7660	1.023	—	—
	50	0.4388	0.5861	42.7	0.427
1	100	0.2971	0.3969	61.2	0.612
	150	0.1891	0.2526	75.3	0.753
	200	0.1240	0.1657	83.8	0.838
	Blank	1.3558	5.432	—	—
	50	0.9165	3.672	32.4	0.324
1.5	100	0.7335	2.938	45.9	0.459
	150	0.6277	2.515	53.7	0.537
	200	0.4555	1.825	66.4	0.664
	Blank	1.720	6.8921	—	—
	50	1.419	5.6859	17.5	0.175
2	100	1.213	4.8637	29.43	0.2943
	150	0.9578	3.8375	44.32	0.4432
	200	0.8260	3.3095	51.98	0.5198

(ηw, %) and corrosion rate (CR_w) are summarized in Table 1. It can be seen from Table 1, that the inhibition efficiency has been considerably increased by increasing the inhibitor concentration of (ACLE) and there is a gradual decrease in corrosion rate. This indicates that the aqueous extract inhibits the corrosion of mild steel in H_2SO_4 and the extent of corrosion inhibition depends on the amount of the extract present.

The inhibition performance of ACLE can be explained as follows [41]:

$$Fe + Inh \leftrightarrow Fe(Inh)_{ads} \leftrightarrow Fe^{n+} + ne^{-} + Inh$$

Initially, when there is not sufficient Fe(Inh)ads to cover the mild steel surface, the extent of metal dissolution takes place in sites free of adsorbat. This because the amount of extract is low or because the adsorption rate is slow.

Correspondingly, the maximum inhibition efficiency obtained at a high concentration of 200 ppm. Further increase in extract concentration did not cause any significant change in the performance of the extract.

When the inhibition performance was monitored in three various concentrations of acid solution, it is observed that the corrosion rate of both in the absence and presence of inhibitor has been increased with the increase in acid concentration. However, Acacia extract showed its best performance in 1M H_2SO_4.

Figure 1 shows the variation of inhibition efficiency of ACLE in the optimal concentration as a function of immersion time. For instance, at 25°C, in the first 4 h immersion, the presence of (ACLE) molecule exerted a negligible influence on the steel dissolution, therefore this compound developed a limited inhibiting action.

It is clear from the same figure that inhibitor efficiency increased with increases immersion time and it reached 83.8% after 24 hours at 25 ±1°C, similarly results obtained by organic compound in 1M H_2SO_4 [42]. Herein, this increase can be explained by the stability and persistence of the inhibitor (ACLE) films adsorbed on the surface [43], which supports the formation of a protective layer, that prevent or minimize the base metal loss and limit the hydrogen liberated.

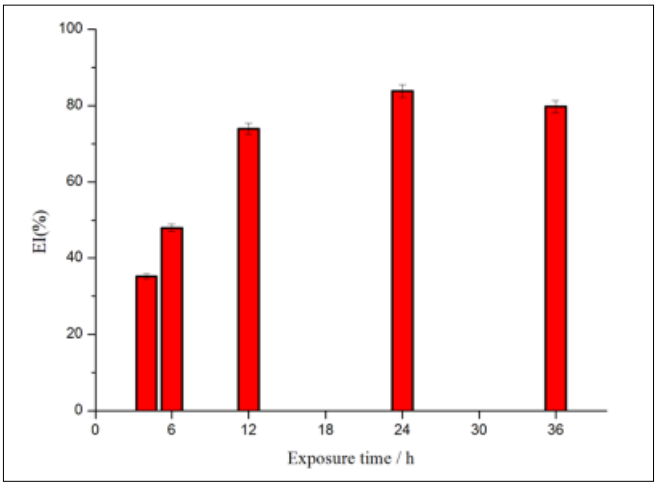

Fig. 1. Variation of the inhibition efficiency as function of immersion time for 200 ppm. ACLE in 1 M H_2SO_4 at 298 K

After 24 h there is a slight decline in the inhibition efficiency at 36 h yielding 79.7%. Prolonged immersion may result in desorption of the extract from mild steel surface [44]. Efficiency initially rises with time and then the absorptive film falls over many days.

3.2. Electrochemical investigation

3.2.1. Open circuit potential

Figure 2 shows the evolution of the open circuit potential (OCP) of mild steel in 1 M H_2SO_4 solution without and with various concentration of (ACLE) after 1800 s of immersion.

It can be observed that the steady state value of OCP firstly moved significantly from –482 mV_{SCE} to the positive direction to –464 mV_{SCE} with the inhibitor concentration increasing from 0 to 100 ppm. Then the potential shifted gradually to the negative direction with further increase in ACLE concentration, and finally reached –471 mV_{SCE} when its concentration is 200 ppm. This result may be interpreted on the bases of the formation of a protective layer of the inhibitor and/or deposition of reaction products on the electrode surface [45].

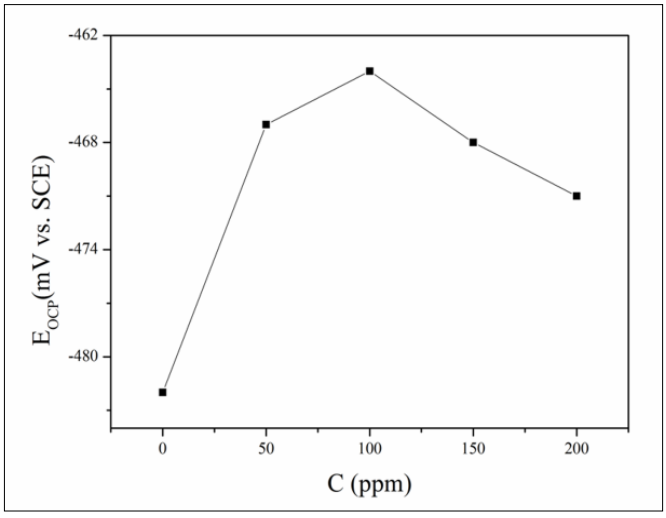

Fig. 2. Steady state OCP values for mild steel immersed in 1 M H_2SO_4 containing (ACLE) with different concentration

3.2.2. Electrochemical impedance spectroscopy measurements (EIS)

EIS technique was used to gain insight into electrochemical processes happening at the steel/acids interfaces in absence and presence of ACLE.

The evaluation of the inhibitory efficiency by Weight loss measurements, the immersion time is of the order of 24 h. In a previous study [32], the inhibitory efficiency by EIS measurements and polarization curves are calculated after 30 min of immersion. This finding leads us to carry out a study of the efficiency after 2 h at OCP.

Impedance spectra of mild steel in 1M H_2SO_4 with and without (ACLE) after 2 h immersion time at OCP are shown in the form of Nyquist plots Fig. 3. The impedance diagram is characterized by one depressed semicircle in both solutions. This behavior indicates that the charge transfer process mainly controls the corrosion of the mild steel [35,46].

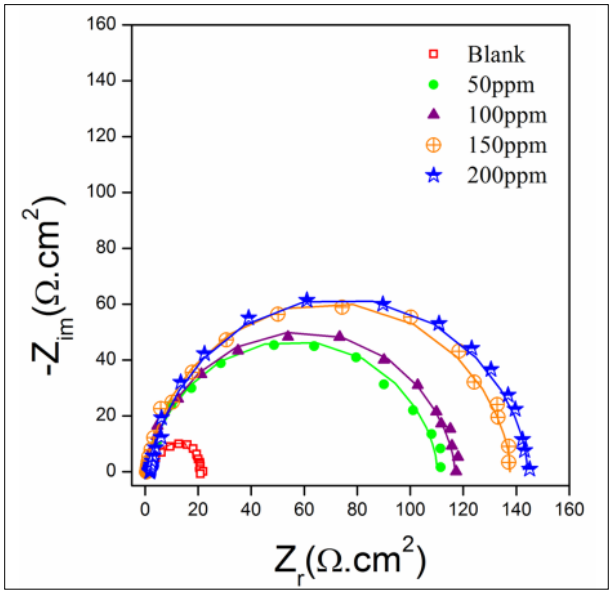

Fig. 3. Nyquist plots of mild steel in 1 M H_2SO_4 containing various concentrations of Acacia extract after 2 h of immersion

Furthermore, the radii of the capacitive semicircle in the presence of ACLE were larger than that registered in blank solution and increases with the inhibitor concentration. This indicates that the impedance of inhibited solution related to various amounts of inhibitor.

In order to extract quantitative information, a nonlinear least squares fit analysis was used to model the spectra, employing electrical equivalent circuits represented in Fig. 4, consisting of a series connection of the resistance R_s with the parallel connection of $R_{ct} - C_{dl}$, is given as:

$$Z(j\omega) = R_s + \frac{Rct}{1 + j\omega C_{dl}.R_{ct}} \tag{9}$$

In fact, the circuit allows the identification of both solution resistance (R_s) and charge transfer resistance (R_{ct}). It can be observed that the impedance loops measured are depressed semi-circles with their centers below the real axis, due to the non-homogeneity or roughness of the electrode surface caused by the corrosion process [47,48], so one constant phase element (CPE) is substituted for the capacitive element to give a more accurate fit in Fig. 4. This circuit was previously used to fit the measured data and to characterize the behavior of steel/acid interface [47,49]. The impedance of the CPE is calculated using the following equation [50,51]:

$$Z_{CPE} = \frac{1}{Q_{dl}(j)^n} \tag{10}$$

In this equation, Q_{dl} represent the magnitude of the CPE, ω is the angular frequency, $j = -1^{1/2}$. If $n = 1$ and n is a measure of non-ideal of the capacitor and has a value in the range of $0 < n < 1$.

The charge transfer resistance, which determines the corrosion rate, must be corresponding to the resistance between the metal and outher Helmholtz plane (OHP). So, the inhibition efficiency (ηi %) is calculated on the basis of the following relation:

$$\eta i = 1 - \frac{R_{ct(0)}}{R_{ct(inh)}} \times 100 \tag{11}$$

Where $R_{ct(0)}$ and $R_{ct(inh)}$ are the charge transfer resistance value without and with inhibitor, respectively.

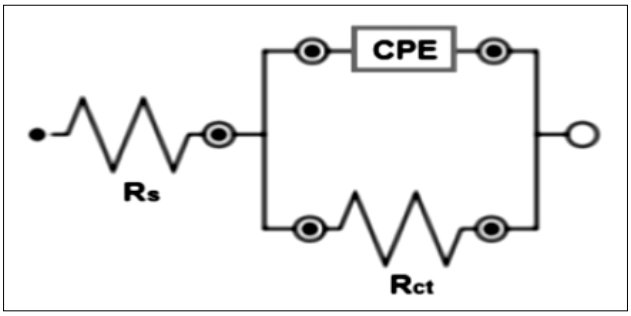

Fig. 4. Electrical equivalent circuit diagram used for modeling the metal/solution interface.

The corresponding values, obtained by fitting the experimental spectra, are presented in Table 2.

TABLE 2

Some parameters obtained from EIS technique used to monitor the inhibition of mild steel corrosion in 1 M H_2SO_4 containing various concentrations of (ACLE)

Inh.C (ppm)	*Rs* ($\Omega.cm^2$)	*Rct* ($\Omega.cm^2$)	CPE_{dl}		ηi (%)
			Q_{dl} ($\mu\Omega.s^n.cm^{-2}$)	*n*	
Blank	0.84206	19.02	583.01	0.8692	—
50	0.8917	110.02	179	0.897	82.71
100	1.278	119.42	142	0.908	84.07
150	1.0228	135.69	130.1	0.910	85.98
200	1.8687	145.80	121	0.918	86.95

Inspection of the results in Table 2 indicated that the value of R_{ct} increases with an increase in ACLE concentration could be attributed to the adsorption of inhibitor compound on the more active site, which effectively blocked the movement of charges across the interface and hence an increase in the inhibition efficiency(ηi) [43].

The average CPE exponent (0.908 ± 0.021) presented in Table 2, thus fulfilling the above requirement. Figure 5 shows the values of n and Q_{dl} vs concentration of Acacia extracts in 1 M H_2SO_4 solution. The low values of Q_{dl} correspond with high values of the n parameter. The addition of ACLE lowers the Q_{dl} values. Thus it can be related to the gradual replacement of water molecules and other ions originally adsorbed on the mild steel

surface by (ACLE) compounds and consequently to a decrease in the number of active sites necessary for the corrosion reaction. This conclusion is in accordance with the findings of other researchers [19,52,53].

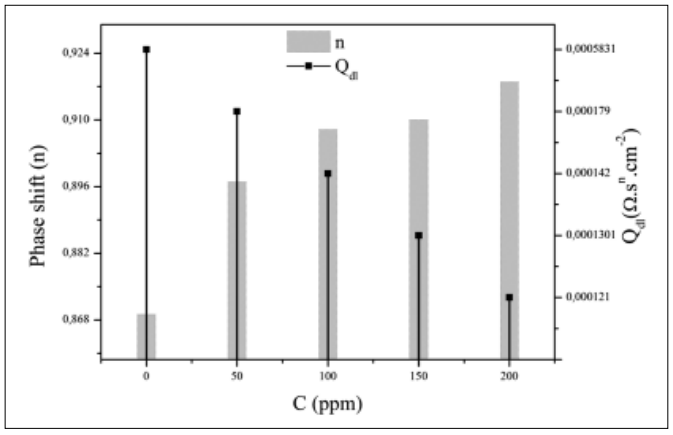

Fig. 5. Phase shift (n) and CPE (Q) values vs concentration (C) of (ACLE) in 1 M H_2SO_4 solution

Moreover, the values of the phase shift (n) increases in presence of ACLE molecules when compared to that obtained in pure 1 (M) H_2SO_4 (0.8692). This can be attributed to a certain decrease in the surface roughness [54], due to the adsorption of the extract molecules on the most active adsorption sites [19]. These results evidenced that Acacia extract protecting mild steel surface from corrosive attack.

The Bode plots also may be easily predicted from the circuit impedance [55]. Let us consider the obtained circuit shown in Figure 4. The phase-angle is described by:

$$\phi = a\tan(Z_{in} / Z_{\mathrm{Re}}) = a\tan\left(\frac{R_{ct}^2\, C_{dl}}{R_s + R_{ct} + (R_{ct}C_{dl})^2 R_s}\right) \quad (12)$$

The phase angle plots and bode impedance are shown in Figure 6a-b respectively.

The phase angle plots indicate a single narrow peak, direct a single time constant at intermediate frequencies Fig. 6a. The mild steel surface roughness increase in the absence of inhibitor therefore reduced the phase angle in the corrosion process. On the opposite side, the presence of (ACLE) compounds on metal effectively lowered surface roughness, as a result phase angle increased approaching to 90° [43]. This confirms the corrosion inhibiting effect of the Acacia extracts.

It is also apparent from Fig. 6b that addition of ACLE causes an increase in the interfacial impedance, which further increases upon increasing concentration of inhibitor. This value is slightly broadened in the optimal concentration of compounds which may suggest the formation of a protective layer [56,57].

The inhibition efficiencies presented in Table 2, show the same trend as those determined from weight loss measurements.

3.3. Adsorption isotherm

The mechanism of inhibition corrosion reactions is studied by adsorption isotherms to understand the adsorption behavior of Acacia extract on mild steel surface.

The adsorption process can be described by two main types of interactions: physical adsorption and chemical adsorption, or both, the type of adsorption depends on the nature and charge of the metal, structure of the extract and the type of electrolyte solution [58]. Among the various isotherms, Langmuir adsorption isotherm is the most fundamental and hence was tested at first.

A straight line was obtained on plotting C_{inh}/θ against C_{inh}, as shown in Figure 7. The obtained plot of the inhibitor was linear and the regression coefficient ($R^2 > 0.998$) suggested that the adsorption of ACLE on mild steel surface fully obeyed to Langmuir isotherm. This Langmuir model has been used for

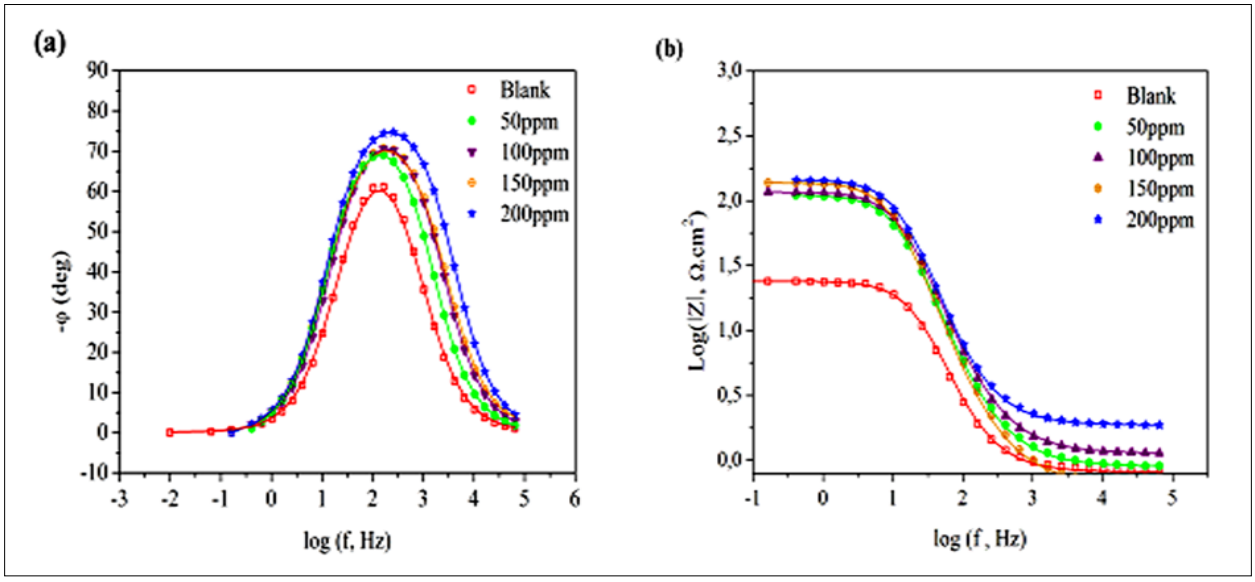

Fig. 6. Bode-phase plots: (a) angle phase and (b) impedance modulus of mild steel in 1 M H_2SO_4 solution with different concentration of ACLE after 2 h immersion .

other inhibitor systems [8,11,59]. According to this isotherm, θ is related to the inhibitor concentration C_{inh}.

$$\theta = \frac{R_{ct(0)} - R_{ct(inh)}}{R_{ct(0)}} \quad (13)$$

$$C_{inh}/\theta = C_{inh} + 1/K_{ads} \quad (14)$$

where C is the equilibrium inhibitor concentration, K adsorptive equilibrium constant, representing the degree of adsorption, which obtained from the reciprocal intercept of Langmuir plot line, and θ is the surface coverage calculated by weight loss measurements.

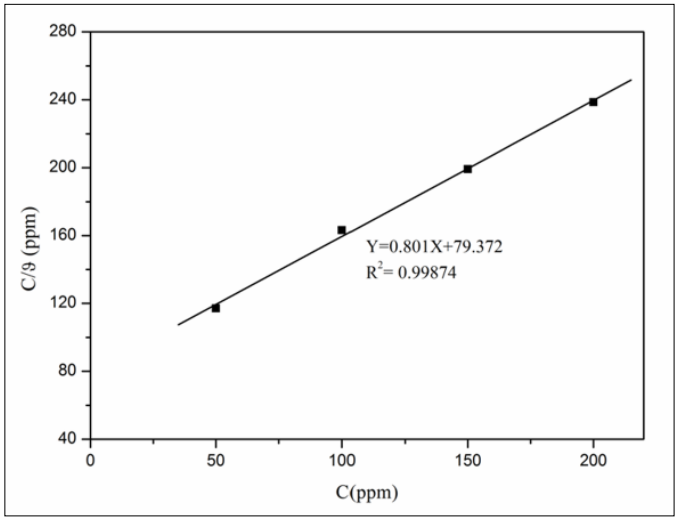

Fig. 7. Plot of Langmuir adsorption isotherm obtained by using surface coverage values calculated by weight loss measurements

The adsorption equilibrium constant related to the free energy adsorption (ΔG_{ads}) can be calculated as below [59]:

$$\Delta G_{ads} = -2.303RT\log(C_{H_2O}\, K_{ads}) \quad (15)$$

Where R is the universal gas constant and T is the absolute temperature.

In the above equation C_{H_2O}= 1.0×10^6 mg.L^{-1} in the solution because unit of K_{ads} has been reported in terms of L mg^{-1}.

The average value of standard adsorption free energy (ΔG_{ads}) was –23.3916 kJ.mol^{-1}. Herein, the negative ΔG_{ads} value evidenced the adsorption process spontaneity and stability of the adsorbed layer on the metal surface [60,61].

Here the calculated $\Delta G°_{ads}$ values are near –20 kJ mol^{-1}; probably means that the adsorption of (ACLE) on mild steel surface is mainly physisorption [48,62].

3.4. FT-IRspectra

To understand the green inhibitors interactions with the metal surface in 1M H_2SO_4, the FTIR spectra were recorded for ACLE inhibitor. Fig. 8a shows a strong broad band at 3380 cm^{-1} is attributed to O-H stretching. The appeared band at 2921.29 and

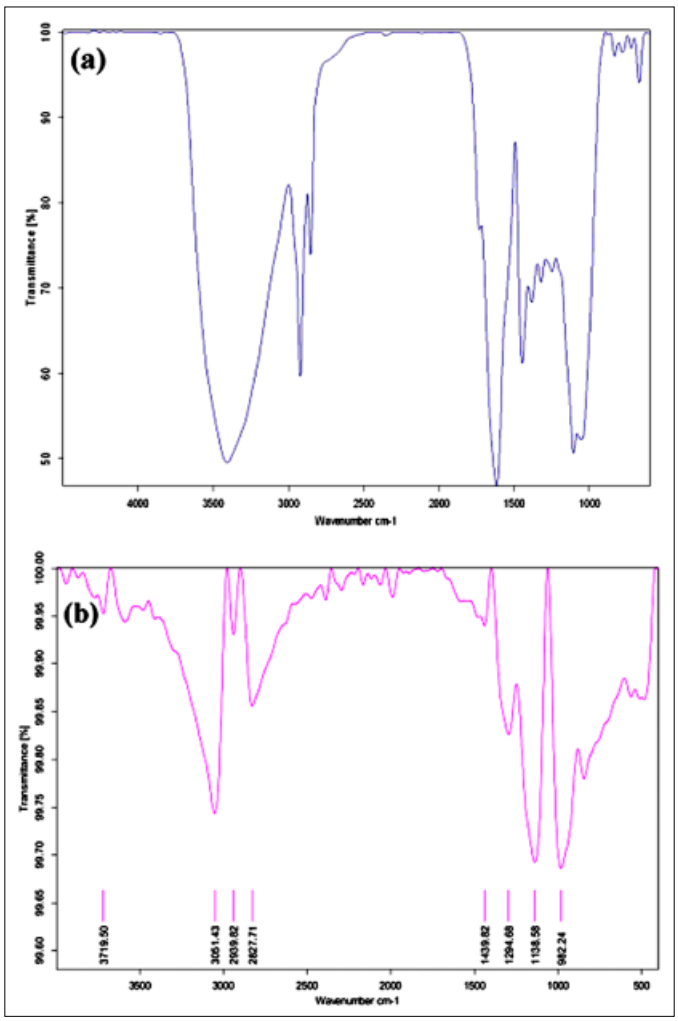

Fig. 8. (a) FT-IRspectrum of inhibitor (b) FT-IRspectrum of inhibitor adsorbed on steel surface

2856.67cm^{-1} are associated to the typical alkanes and aromatics C-H stretch. At 1640 cm^{-1}, a very strong band is assigned to C = C and C = O stretching vibration. C = C and C = O stretching vibration bands are superposition [63,64]. The flavonoids conjugation effect of ACLE showed a slight shifts of the C = O peak (1700 cm^{-1}) towards lower wavenumber (1640 cm^{-1}). Additionally, the observed bands at 1459.20 cm^{-1} and 765.23 cm^{-1} are associated to the C-H scissoring/streatching and the aromatic stretching vibration, respectively.

For the appeared band at 1101 and 1088 cm^{-1}, this corresponds to the aromatic ring carbonyl C-O and C-O for primary alcohol, respectively and reflected band of aromatic ring carbonyl appeared at 660 cm^{-1}. These observations are in agreement with that reported by EL Sissi and co-workers [30], and consistent with the bonds that make up flavonoids are the main components present in ACLE. In Fig. 8b, the IR spectrum of a scraped sample shows two weak bands at 3786.71 and 3719.50 cm^{-1} which do not appear in Fig. 8a are assigned to Fe-O bending [65,66], which reveal the fact that Acacia extract can adsorb on the metal surface on the basis of donor-acceptor interactions between lone-pair electrons of oxygen and the vacant d-orbital of Fe substrate.

The presence of Acacia extract over the complex surface was evidenced by the low intensity characteristic bands of C-H from CH_2 and CH_3 at 2939.82, 2871.71, 1462, and 1439.82 cm^{-1} [67,68].

The band corresponding to C = C at 1640 cm^{-1} disappeared due to the interaction of π electrons of aromatic rings with mild steel surface [69] .

The two vibrations at 1101 and 1088 cm^{-1} corresponding to C-O disappeared, and it is observed from figure 8b, the presence of other bands may be original oxide between (720 and 1294.68 cm^{-1}) initially formed on the surface of the steel.

This result suggests that there is an interaction between the ACLE molecule and the surface of mild steel.

3.5. Atomic Force Microscopy (AFM)

AFM is a powerful technique to investigate the surface morphology at nano- to micro-scale [66,70].

Three Three-dimensional AFM images for mild steel after immersion in 1 M H_2SO_4 without and with 200ppm of aqueous Acacia Extract are shown in Figure 9a-b, respectively.

As can be seen from Fig. 9a, the corrosion of mild steel samples in the absence of inhibitor appeared to be relatively uniform in general. The sample surface is badly damaged due hydrogen atoms that enters the metal produces some detrimental effects on the mechanical properties of mild steel surface. On the other hand, in the presence of ACLE inhibitor, Fig. 9b shows that the mild steel surface appears more flat and homogeneous, this indicated that ACLE shows an appreciable resistance to corrosion.

Fig. 10a-b illustrates the height profiles of the sample in 1M H_2SO_4 without and with inhibitor respectively.

Fig. 10a shows that the surface roughness of the mild steel in uninhibited 1.0 M H_2SO_4 is about 61.41 nm, while in the presence of ACLE, the roughness decreases to 36.7 nm (Fig. 10b). Thus, the roughness is consistent with the results shown in Figs. 9a-b.

The decrease in the roughness is attributed to the formation/ adsorption of a protective layer of Fe^{2+}-ACLE complex on the

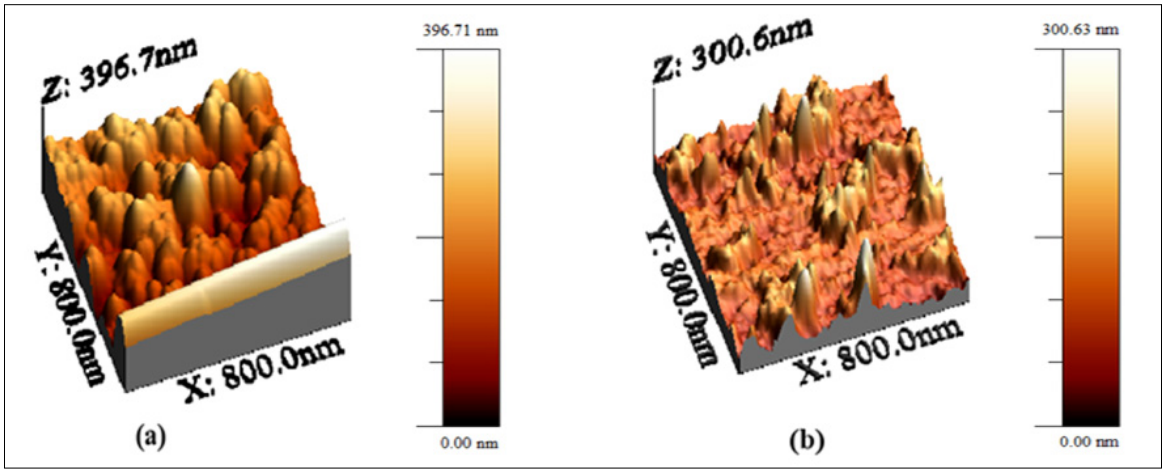

Fig. 9. AFM three-dimensional images of the mild steel surface in 1.0 M H2SO4: (a) in the absence of inibitor; (b) in the presence of 200 ppm after immersion time of 24h. Scan area: 800 nm × 800 nm

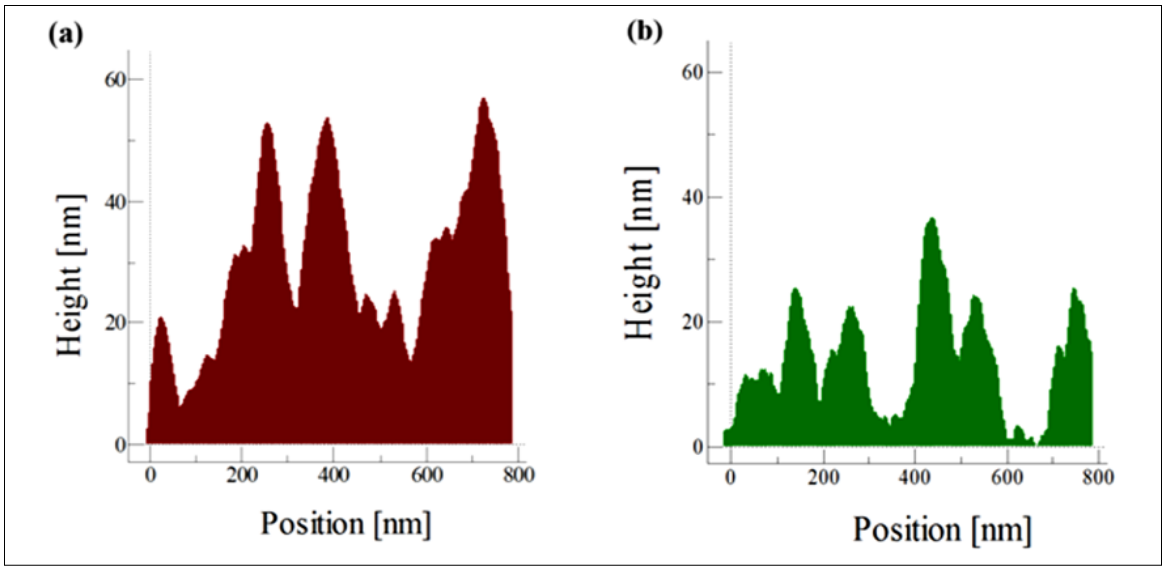

Fig. 10. Height profiles of the mild surface in 1.0 M H_2SO_4: (a) in the absence of inhibitor; (b) in the presence of 200 ppm. Scan area: 800 nm × 800 nm

metal surface as revealed initially by FT-IR spectrum and weight loss measurements. However, the presence of ACLE inhibitor alone in the solution not being enough to form a uniform film. It may be deduced that addition of other additive in the solution is necessary to get uniform film, which leads to a higher inhibition efficiency.

3.6. Corrosion inhibition mechanism

FTIR results of the ACLE showed the presence of oxygen atoms in functional groups (O-H, C=O, C-O), that may come from the hydrocarbons and aromatic rings from phytoconstituents of the extracts.

From the experimental and theoretical results obtained, the natural compounds in ACLE molecules will be protonated in acid solution [57,71]:

$$ACLE + xH^{+} \leftrightarrow [ACLEH_x]^{x+} \quad (16)$$

It is also well known that $SO4^{2-}$ ions are strongly adsorbed in acid medium on the metal surface leaving less space available for organic molecules to adsorb [72,73].

In presence of SO_4^{2-} ions, the following rapid reaction proceeds on the mild steel surface:

$$H_2O_{ads} + SO_4^{2-} = SO_4^{2-}{}_{ads} + H_2O \quad (17)$$

The substitution of water molecules with SO_4^{2-} ions leads to creating an excess negative charge on surface, which in turn, facilitates physical adsorption of the protonated form $[ACLEH_x]^{x+}$ through electrostatic interactions between positively charged inhibitor and negatively charged mild steel surface [74,75]. However, the exact mechanism of corrosion inhibition could not be envisaged due to unspecified molecular weight of the extracts. So when protonated chemical molecules in Acacia extract are adsorbed on steel surface and release of H_2 gas, a coordinate bond may be formed by the presence of aromatic ring (source p electrons) or oxygen atom (non bonding electrons) from the neutral form confirmed by FTIR, which could activate formation of a chemical bond with vacant d-orbital electrons of charged steel surface to form the metal inhibitor complexes:

$$Fe \rightarrow Fe^{2+} + 2e^{-} \quad (18)$$

$$ACLE + Fe^{2+} \leftrightarrow [ACLE - Fe]^{2+} \quad (19)$$

$$[ACLEH_x]^{x+} + Fe^{2+} \leftrightarrow [ACLEH_x - Fe]^{(2+x)+} \quad (20)$$

These complexes might get adsorbed onto steel surface by van der Waals force to form a protective film which keeps mild steel during pickling acid process without significantly affecting the rate of oxide removal [63].

AFM results prove that Acacia extract could adsorb onto mild steel surface to form a denser and more tightly protective film.

3.7. Comparative study of (ACLE) inhibitor with some chemical pickling inhibitor

The comparison of inhibition efficiency of (ACLE) inhibitor with a standard cleaning solution for mild steel immersed in dilute H_2SO_4 solution at room temperature clearly proves the result obtained. It is postulated that the double or triple bond is more toxic than a steric hindrance bond. A double or triple bond react significantly faster and hence make them eligible for direct interactions with the biochemical macromolecules, result in a number of catastrophic effects. It is important to note, for example a,b-unsaturated carbonyl or carboxyl fragment are very important in the manufacture of polymers, textiles, or auxiliary materials in medicine [76].

In the case of standard pickling solution [77] for mild steel, about 84 mg of toxic chemicals such as 2-Methyl-3-Butun-2-ol was used in 1L of dilute H_2SO_4. It is worth mentioning that the corrosion rate and inhibition efficiency at low concentration (50 ppm) of (ACLE) compounds are comparable with that of standard cleaning solution [78,79]. Regarding toxicity, the 50 Lethal Concentration (LC50) value of standard inhibitor is 1950 $mg.kg^{-1}$, whereas the LD50 value of A. Cyanophylla is 25,000 $mg.kg^{-1}$ [80] which is explicit that ACLE inhibitor is around 13 times less toxic than the chemical inhibitor. The decisive of triple bonds of acetylenic alcohol molecules due to the p-electrons interaction with the metallic surfaces is generally accepted [68], but this bonds increases its toxicity [81]. Furthermore, according to Podobaev and Avdeev, the scale of toxic rating acetylenic alcohols falls under “practically toxic” category [82].

Hence, the natural inhibitor A. Cyanophylla extracts can be an alternative to the toxic chemicals in pretreatment processes. Also correct additive selection is important to guarantee minimum adverse effects on environments and human health with satisfactory corrosion inhibition efficiency.

4. Conclusions

In summary, the ACLE can act as an effective inhibitor for the corrosion of steel in 1 M H_2SO_4. The inhibition efficiencies vary linearly with concentration and immersion time until one day. The optimum value was found at 200 ppm for 24 h immersion at 298 K.

The inhibition efficiency increased with increase in inhibitor concentration and immersion time, however decreased with acid concentration. The optimum value was found at 200 ppm of Acacia extract for 24 h immersion in 1 M H_2SO_4 at 298 K.

Impedance studies revealed that the inhibitors reduced the corrosion rate by increasing the resistance of the system.

The adsorption of ACLE on mild steel surface was found to accord with Langmuir adsorption isotherm model. The free energy indicates that the adsorption of extract involves mainly the physical adsorption. Additionally, AFM studies supported the formation of a smooth surface on mild steel in the presence

of Acacia Cyanophylla extract compounds probably due to the formation of an adsorptive film. These results are in agreements with the FTIR results.

Laboratory results from this study suggest that the ACLE is a potential eco-friendly corrosion inhibitor, which may be beneficial for steel pickling process. Also of importance is the exploration of ACLE in other corrosive environment such as CO_2 corrosion, H_2S corrosion and in cooling water systems.

REFERENCES

[1] K.P. Vinod, M.S. Narayanan, G.R. Thusnavis, J. Mater. Sci. **46**, 5208-5215 (2011).

[2] A. Chekioua, R. Delimi, Energy Procedia. **74**,1418 -1433 (2015).

[3] E. Kowsari, M. Payami, R. Amini, B. Ramezanzadeh, M. Javanbakht, Appl. Surf. Sci. **289**, 478-486 (2014).

[4] S. Issaadi, T. Douadi, A. Zouaoui, S. Chafaa, M.A. Khan, G. Bouet, Corros. Sci. **53**, 1484-1488 (2011).

[5] J. Aljourani , M.A. Golozar, K. Raeissi, Mater. Chem. Phys. **121**, 320-325 (2010).

[6] N. Etteyeb, X.R. Nóvoa, Corros. Sci. **112**, 471-482 (2016).

[7] N.O. Eddy, P.A. Ekwumemgbo, P.A.P. Mamza, Green Chem. Lett. Rev. **2**, 223-231 (2009).

[8] S.A. Umoren, J. Adhes. Sci. Technol. **30**, 1858-1879 (2016).

[9] Z.V.P. Murthy, K. Vijayaragavan, Green. Chem. Lett. Rev. **7**, 209-219 (2014).

[10] K.K. Anupama, K.M. Shainy, A. Joseph, J. Bio. Tribo. Coroos. **2**, 2 (2016).

[11] I. Ikeuba, B.I. Ita, P.C. Okafor, B.U. Ugi, E.B. Kporokpo, Prot. Met. Phys. Chem. Surf. **51**, 1043-1049 (2015)

[12] Y.M. Khaburs'kyi, Materials Science. **51**, 131-137 (2015).

[13] P. Slepski, H. Gerengi, A. Jazdzewska, J. Orlikowski, K. Darowicki, Constr. Build. Mater. **52**, 482-487 (2014).

[14] E.E. Ebenso, H. Alemu, S.A. Umoren, I.B. Obot, Int. J. Electrochem. Sci. **3**, 1325-1339 (2008).

[15] E.E. Ebenso, E.E. Oguzie, Mater. Lett. **59**, 2163-2165 (2005).

[16] G.H. Booth, S.J. Mercer , Corros. Sci. **4,** 425 (1964).

[17] A.A. Rahim, E. Rocca, J. Steinmetz, M.J. Kassim, R. Adnan, M.S. Ibrahim, Corros. Sci. **49**, 402-417 (2007).

[18] M. Oki, E. Charles, C. Alaka, T.K. Oki, Mater. Sci. Appl. **02**, 592-595 (2011).

[19] H. Gerengi, A. Jazdzewska, M. Kurtay, J. Adhes. Sci. Technol . **29**, 36-48 (2015).

[20] N.A.A. Talib, S. Zakaria, C.C. Hua, N.K. Othman, AIP Conf. Proc. **1614** , 171-177 (2014).

[21] R.T. Lange, J. Microbiol. Serol. **25**, 272 (1959).

[22] J. Clark-Lewis, I. Dainis, Aust. J. Chem. **20,** 2191-2198 (1967)

[23] World Bank, A Strategy for the Development a course in arid and Semi Arid area, Annex III Technical Report, 1995, 162,Tunisia.

[24] N. Lassoued, M. Rekik, H. Ben Salem, M.A. Dargouth, Livest. Sci. **105**, 129-136 (2006).

[25] S.A. Sotohy, A.N. Sayed, M.M. Ahmed, DTW. Dtsch. Tierztl. Wochenschr. **104**, 432 (1997).

[26] A.A. Dafallah, Z. Al-Mustafa, Am. J. Chin. Med. **24**, 263 (1996).

[27] G. Avci, Y. KeleŞ, Surf. Interface Anal. **43**, 1311-1317 (2011).

[28] N.M. Gumgumjee, A.S. Hajar, Int. J. Microbiol. Immunol. Res. **3**, 51-57 (2015).

[29] Paris, R. R. Bull. Sot C&mBbi. **35**, 655 (1953).

[30] H.I. El Sissi, A.E. El Sherbeiny, Qual. Plant. Mater. Veg. **14**, 257 (1967).

[31] E. Haslam, J. Nat. Prod. **59**, 205-215 (1996).

[32] M. Tezeghdenti, N. Etteyeb, L. Dhouibi, O. Kanoun, A. Al-Hamri, Protection of Metals and Physical Chemistry of Surfaces. **53**, 753-764 (2017).

[33] H. Ashassi-Sorkhabi, M.R. Majidi, K. Seyyedi, Appl. Surf. Sci. **225**, 176 (2004).

[34] S.D. Deng, X.H. Li, H. Fu, Corros. Sci. **53**, 760-768 (2011).

[35] N.O. Obi-Egbedi, I.B. Obot, Arab. J. Chem. **6**, 211-223 (2013).

[36] M. Prajila, A. Joseph, J, Bio, Tribo, Corros. **3**,10 (2017).

[37] N.I. Kairi, J. Kassim, Int. J. Electrochem. Sci. **8**, 7138-7155 (2013).

[38] A. Chattopadhyay, N. Bandyopadhyay, A.K. Das, M.K. Panigrahi, Scr. Mater. **52**, 211-215 (2005).

[39] Z. Panossian, N.L.d. Almeida, R.M.F.d. Sousa, G.d.S. Pimenta, L.B.S. Marques, Corros. Sci. **58**, 1-11 (2012).

[40] N. Raghavendra, J. Ishwara Bhat, J. Bio. Tribo. Corros. **4**, 2 (2018).

[41] A.K. Singh, M. . Quraishi, J. Appl. Electrochem. **40**, 1293-1306 (2010).

[42] A. Spinelli, R.S. Gonçalves, Corros. Sci. 30, 1235-1246 (1990).

[43] M.A. Quraishi, D. Jamal, Anti. Corros. Method. M. 47, 233-240 (2000).

[44] S.K. Shukla, M.A. Quraishi, Corros. Sci. **52**, 314-321 (2010).

[45] E.E. Oguzie, Y. Li, F.H. Wang, Electrochim. Acta. **53**, 909-914 (2007).

[46] N. D. Gowraraju, S. Jagadeesan, K. Ayyasamy, L.O. Olasunkanmi, E.E. Ebenso, S. Chitra , J. Mol. Liq. **232**, 9-19 (2017).

[47] S.D. Deng, X.H. Li, Corros. Sci. **55**, 407-415 (2012).

[48] A. Rodríguez-Torres, O. Olivares-Xometl, M.G. Valladares-Cisneros, J.G. González-Rodríguez, Int. J. Electrochem. Sci. **13**, 3023-3049 (2018).

[49] M. Chevalier, F. Robert, N. Amusant, M. Traisnel, C. Roos, M. Lebrini, Electrochim. Acta. **131**, 96-105 (2014).

[50] A.K. Singh, E.E. Ebenso, Res. Chem. Intermed. **39**, 1823-1831 (2013).

[51] M.H. Hussin, M.J. Kassim, Mater. Chem. Phys. **125**, 461-468 (2011).

[52] S.A. Umoren, I.B. Obot, Z. Gasem, N.A. Odewunmi, J. Dispers. Sci. Technol. **36**,789-802 (2014).

[53] S.S. Abd El-Rehim, M.M. Deyab, H.H. Hassan, A.A. Ibrahim, Z. Phys. Chem. **230**, 1641-1653 (2016).

[54] J.O.L. Riggs, Second ed. C.C, (1973) Nathan, Houston TX.

[55] J.J. DiStefano, A.R. Stubberud, I.J. Williams, Theory and Problems of Feedback and Control Systems: 2nd. ed., Schaum's Outline Series, 1990 McGraw-Hill, New York.

[56] C.B. Verma, M.A. Quraishi, E.E. Ebenso, Int. J. Electrochem. Sci. **8**, 12894-12906 (2013).

[57] D.K. Yadav, D.S. Chauhan, I. Ahamad, M.A. Quraishi, RSC Advances **3**, 632 (2013).

[58] S.A. Umoren, E.E. Ebenso, Mater. Chem.Phys. **106**, 387-393 (2007).

[59] N. Goudarzi, M. Peikari, M.R. Zahiri, H.R. Mousavi, Arch. Metall. Mater. **57**, 845-851 (2012).
[60] P. Muthukrishnan, B. Jeyaprabha, P. Prakash, Acta Metall. Sin. **26**, 416-424 (2013).
[61] S.A. Umoren, I.B. Obot, E.E. Ebenso, P.C. Okafor, O. Ogbobe, E.E. Oguzie, Anti-Corros. Met. Mater. **53**, 277-282 (2006).
[62] A.S. Fouda, K. Shalabi, A. E-Hossiany, J. Bio. Tribo. Corros. **2**, 18 (2016).
[63] X.H. Li, S.D. Deng, H. Fu, Corros. Sci. **62**, 163-175 (2012).
[64] H. Cang1, Z. Fei, H. Xiao, J. Huang, Q. Xu, Int. J. Electrochem. Sci. **7**, 8869-8882 (2012).
[65] X.H. Li, S.D. Deng, H. Fu, J. Appl. Electrochem. **40**, 1641-1649 (2010).
[66] Q. Qu, S.A. Jiang, W. Bai, L. Li, Electrochim. Acta. **52**, 6811(2007).
[67] M. Gojic, L. Kosec, J. Iron Steel Inst. Int. **37**, 685-690 (1997).
[68] C. Fiaud, A. Harch, D. Mallouh, M. Tzinmann, Corros. Sci. **35**, 1437-1444 (1993).
[69] K. Chennappan, G.S. Mathur Gopalakrishnan, Ind. Eng. Chem. Res. **51**, 10399-10407 (2012).
[70] S. Perumal, S. Muthumanickam, A. Elangovan, R.Karthik, R. Sayee kannan, K.K. Mothila, J. Bio. Tribo. Corros. **3**, 13 (2017)
[71] M. Tezeghdenti, L. Dhouibi, N. Etteyeb, J. Bio. Tribo. Corros. **1**, 16 (2015).
[72] F. Bentiss, M. Traisnel, M. Lagrenee, Corros. Sci. **42**, 127-146 (2000).
[73] R. Solmaz, M.E. Mert, G. Kardaş, B. Yazici, M. Erbıl, Acta Phys--Chim. Sin. **24**, 1185-1191 (2008).
[74] A.K. Singh, V.K. Singh, M.A. Quraishi, Int. J. Corros. 2010 (2010).
[75] L. Elkadi, B. Mernari, M. Traisnel, F. Bentiss, M. Lagreneée, Corros. Sci. **42**, 703-719 (2000).
[76] D.W. Potter, T.B.Tran, Toxicol. Lett. 62, 275-285 (1992).
[77] ASTM Standards, Corrosion of Metals: Wear and Erosion, 1995, USA.
[78] A. Frignani, C. Monticelli, F. Zucchi , G. Trabanelli, Int. J. Corros. Scale Inhib. **3**, 105-119 (2014).
[79] Y.G. Avdeev, Y.I. Kuznetsov, Russ. Chem. Rev. **81**, 1133 (2012).
[80] F. Yousif, M.S. Hifnawy, G. Soliman, L. Boulos, T. Labib, S. Mahmoud, F. Ramzy, M. Yousif, I. Hassan, K. Mahmoud, S.M. El--Hallouty, M. El-Gendy, L. Gohar, M. El-Manawaty, W. Fayyad, B.S. El-Menshawi, Pharm. Biol. **45**, 501-510 (2008).
[81] S.H. Zaferani, M. Sharifi, D. Zaarei, M.R. Shishesaz, J. Environ. Chem. Eng. **1**, 652-657 (2013).
[82] N.I. Podobaev, Y.G. Avdeev, Prot. Met. **40**, 7-13 (2004).